Optimization of the Conical Angle Design in Conical Implant-Abutment Connections: A Pilot Study Based on the Finite Element Method

Article *in* Journal of Oral Implantology · November 2017

DOI: 10.1563/aaid-joi-D-17-00149

CITATIONS
4

READS
852

7 authors, including:

Yao Kuang-Ta
National Yang Ming University
11 PUBLICATIONS **66** CITATIONS
SEE PROFILE

Chen-Sheng Chen
National Yang Ming University
59 PUBLICATIONS **1,595** CITATIONS
SEE PROFILE

Cheng-Kung Cheng
Shanghai Jiao Tong University
313 PUBLICATIONS **4,688** CITATIONS
SEE PROFILE

Hsu-Wei Fang
National Taipei University of Technology
113 PUBLICATIONS **1,306** CITATIONS
SEE PROFILE

Optimization of the Conical Angle Design in Conical Implant–Abutment Connections: A Pilot Study Based on the Finite Element Method

Kuang-Ta Yao, DDS, PhD[1]
Chen-Sheng Chen, PhD[2]
Cheng-Kung Cheng, PhD[3]
Hsu-Wei Fang, PhD[4]
Chang-Hung Huang, PhD[5]
Hung-Chan Kao, PhD[3]†
Ming-Lun Hsu, DrMedDent[6]*†

Conical implant–abutment connections are popular for their excellent connection stability, which is attributable to frictional resistance in the connection. However, conical angles, the inherent design parameter of conical connections, exert opposing effects on 2 influencing factors of the connection stability: frictional resistance and abutment rigidity. This pilot study employed an optimization approach through the finite element method to obtain an optimal conical angle for the highest connection stability in an Ankylos-based conical connection system. A nonlinear 3-dimensional finite element parametric model was developed according to the geometry of the Ankylos system (conical half angle = 5.7°) by using the ANSYS 11.0 software. Optimization algorithms were conducted to obtain the optimal conical half angle and achieve the minimal value of maximum von Mises stress in the abutment, which represents the highest connection stability. The optimal conical half angle obtained was 10.1°. Compared with the original design (5.7°), the optimal design demonstrated an increased rigidity of abutment (36.4%) and implant (25.5%), a decreased microgap at the implant–abutment interface (62.3%), a decreased contact pressure (37.9%) with a more uniform stress distribution in the connection, and a decreased stress in the cortical bone (4.5%). In conclusion, the methodology of design optimization to determine the optimal conical angle of the Ankylos-based system is feasible. Because of the heterogeneity of different systems, more studies should be conducted to define the optimal conical angle in various conical connection designs.

Key Words: conical implant–abutment connection, conical angle, nonlinear finite element analysis, design optimization, Ankylos implant system, abutment fracture

INTRODUCTION

In recent years, the use of dental implants has become a reliable treatment modality for single-tooth restorations because of the well-documented high success rate of osseointegration.[1,2] Nevertheless, the longevity of implant therapy remains a critical concern. Biological and mechanical complications, such as crestal bone resorption and screw loosening, are particularly problematic.[3,4] Both are related to the connection. To be more specific, there is an inevitable microgap in the connection between an implant and an abutment, which tends to result in bacterial accumulation and stress concentration. A direct correlation between misfit and joint instability was proven, and the misfit should be minimized.[5,6]

Conical implant–abutment connections have been developed and have become popular because of the perfect stability that is achieved through implant–abutment connections, which reduces the incidence of the aforementioned complications.[7–9] The efficient clinical performance of conical connections is attributable to their large clamping force, which is transformed from the large frictional resistance in the conical interface and helps 2-piece connections function as a single entity.[10,11]

In terms of the conical connection mechanism, frictional resistance originates from the geometric characteristic of the cone in the connection, allowing the abutment to sink into the implant bore. Theoretically, the degree of the conical angle can

[1] Department of Dentistry, National Yang-Ming University, Taipei, Taiwan.
[2] Institute of Rehabilitation Science and Technology, National Yang-Ming University, Taipei, Taiwan.
[3] Department of Biomedical Engineering and Orthopaedic Device Research Center, National Yang-Ming University, Taipei, Taiwan.
[4] Department of Chemical Engineering and Biotechnology & Institute of Chemical Engineering, National Taipei University of Technology, Taipei, Taiwan; Division of Medical Engineering Research, National Health Research Institutes, Miaoli, Taiwan.
[5] Department of Medical Research, Mackay Memorial Hospital, Taipei, Taiwan.
[6] School of Dentistry, National Yang-Ming University, Taipei, Taiwan.
* *Corresponding author,* e-mail: mlhsu@ym.edu.tw
† These authors contributed equally to this work.
DOI: 10.1563/aaid-joi-D-17-00149

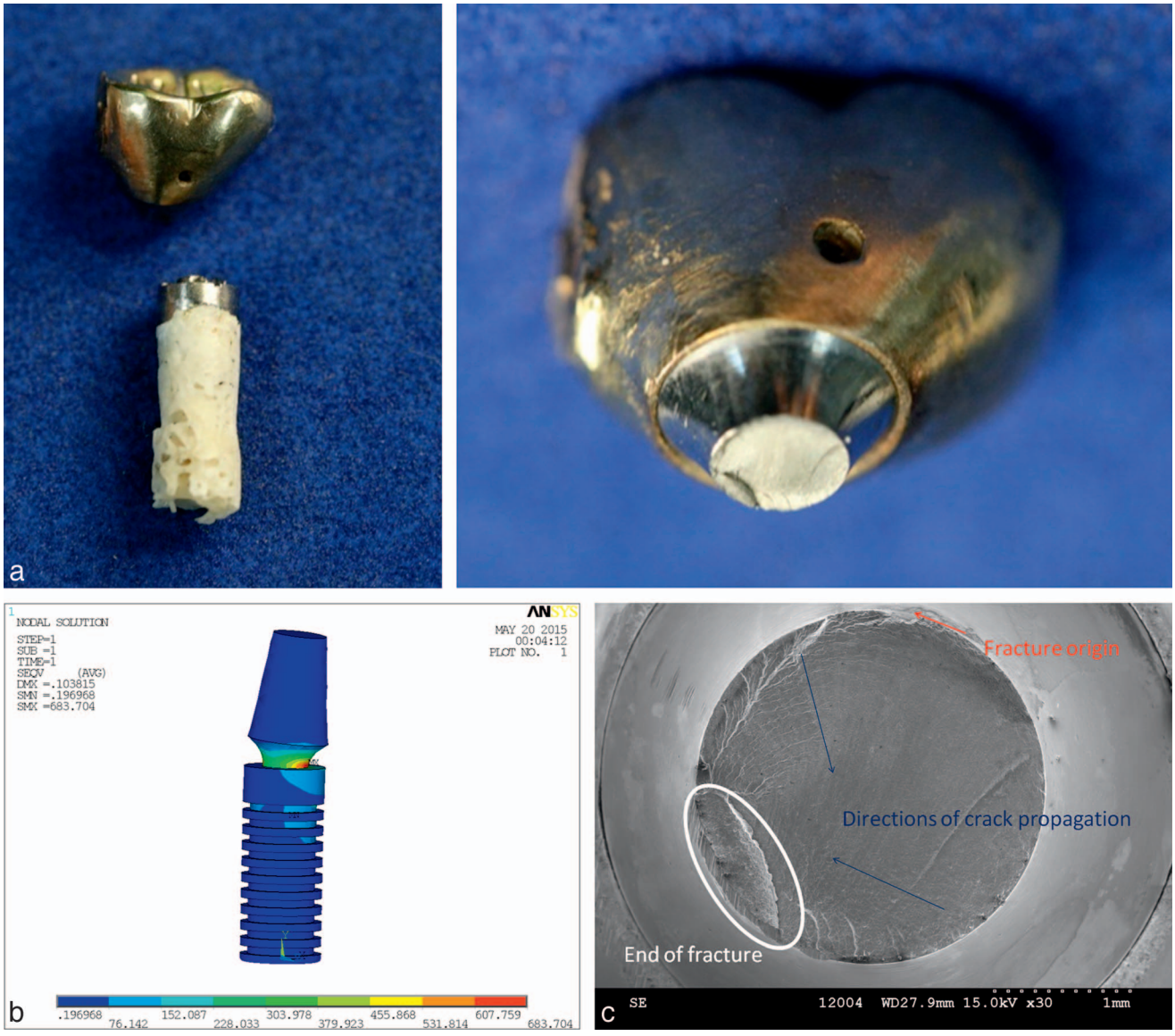

Figure 1. Photographs, scanning electron microscopy examination results, and finite element analysis results of a retrieval case. (a) The clinical failure case demonstrated that the abutment fractured at the implant platform level. The implant body was removed with trephines. (b) The corresponding finite element analysis demonstrated that maximum von Mises stress occurred in the abutment at the implant platform level, consistent with the clinical findings in (a). (c) Scanning electron microscopy observations of the fracture surface demonstrated that the end of the fracture was not exactly opposite the fracture origin and that the directions of the crack propagation were multiple. These findings indicated that the abutment withstood not only bending forces but also torsional forces.

directly control the amount of frictional resistance.[12,13] A smaller conical angle leads to greater frictional resistance, and consequently benefits the connection stability. However, a smaller conical angle also results in reduced abutment rigidity, which compromises the connection stability. In other words, the conical angle exerts opposing effects on 2 influencing factors crucial to connection stability: frictional resistance and abutment rigidity. Clinically, the conical angles vary in different conical connection implant systems, and little information on this topic is available.

With increasing significance, several clinical failure cases have reported that all abutment fractures of the Ankylos implant system (Dentsply-Friadent GmbH, Mannheim, Germany), a reliable conical implant–abutment connection system,[14,15] occurred horizontally at the implant platform level (Figure 1a). This was originally considered an uncomplicated clinical problem solvable by exchanging a new abutment. However, the large clamping force from its distinctive frictional resistance in the connection made retrieving the fracture abutment difficult, thereby the aggressive treatment of implant body removal with trephine as a final solution. Accordingly, we analyzed these failed retrieval cases to investigate the possible causes of failure and the influencing factors.

One of the common characteristics of these cases was that all the failures occurred in posterior single implant restorations after 1 to 2 years of service. In addition, scanning electron

microscopy observations of fractured surfaces demonstrated that the failure patterns had the characteristics of fatigue in ductile materials under not only the bending forces but also the torsional forces originating from chewing (Figure 1c). From these observations, it can be assumed that the actual cause of these failures is weakness in the rigidity of the abutment, which is thus unable to withstand the bending and torsional forces in the posterior areas. Our findings are consistent with a finite element analysis (FEA) study warning that the reduced abutment diameter of the Ankylos system, originating from its small conical angle, may increase the risk of abutment fracture.[16] Elsewhere, a Korean clinical study demonstrated a similar concern, reporting that the incidence of abutment fracture of the Ankylos implant system in the Korean population was up to 2.2%.[17] In addition, difficulty in retrieval was encountered. In brief, the conical angle in this system, simultaneously controlling the abutment rigidity and frictional resistance with opposing effects on the connection stability, appears to overemphasize the frictional resistance and neglect the abutment rigidity. Consequently, this leads to the difficult clinical situation in which the abutments fracture and the fracture fragments are too tight to be retrieved.

From a mechanical engineering perspective, directly increasing the conical angle to increase the abutment diameter and thereby increase abutment rigidity appears to be a feasible solution to mitigate this retrieval problem. However, because occlusal loading is exerted on the whole conical implant–abutment connection rather than on the abutment alone, increasing the abutment rigidity is not sufficient to prevent abutment fracture; instead, the rigidity of the whole connection (ie, the connection stability), should be increased. The higher the connection stability, the smaller and more favorably distributed the stress in the abutment is, which thus contributes to a lower abutment fracture possibility. In sum, the stress condition in the abutment is a valid indicator of the connection stability.

Because the conical implant–abutment connection comprises the abutment, corresponding implant wall confining the abutment, and clamping force (frictional resistance) within the connection, the rigidity of the corresponding implant wall also affects the connection stability. Furthermore, changes in the conical angle cause different changes in the aforementioned factors of connection stability and differently affect connection stability. Increasing the conical angle increases the abutment diameter and, consequently, the connection stability. However, the thickness of the corresponding implant wall decreases as a result of the increased abutment diameter, and the clamping force within the conical connection also decreases as a result of the increase in conical angle.[12,13] Both of these effects reduce the connection stability. Therefore, from an engineering design perspective, an optimal conical angle should be determined by mediating these 3 factors. Using a scientific methodology, the present study calculated this optimal conical angle.

Computer technology has contributed to product design, analysis, and manufacturing. First, computer-aided engineering, the use of computer software to improve product quality and durability, is widely applied. One key element of computer-aided engineering, FEA, is mostly used to evaluate and refine product designs through computer simulations rather than physical prototype testing, thus saving time, efforts, and money.[18–20] Second, digital scanning and computer-aided design (CAD) technologies can be applied to the construction of simulation models.[21–23] Third, computer-aided manufacturing (CAM) technology can be used to produce solid models. Currently, digital scanning, CAD technologies, and CAM technologies are also used to fabricate prostheses in clinical dental practice.

A parametric design optimization approach through FEA can be used to obtain the optimal parameter by using a series of optimization iterations. Furthermore, FEA is an effective simulation tool for solving design challenges without arduous manual iterations or prototyping. The ANSYS FEA package (ANSYS Inc, Canonsburg, Pa) has a powerful design optimization module in structural design optimizations.[24] In addition, ANSYS Parametric Design Language, a scripting language that can be used to build a model in terms of variables, was used to build a model parametrically to enable variable changes during the optimization process. This process systematically and efficiently adjusts the influencing parameters to determine the solution with the optimal performance, satisfying given constraints. The optimization can be represented by the following mathematical mode:[25]

$$\begin{array}{ll} \textit{Minimize} & f(x) \\ \textit{Subject to} & S_i^L \le s_i(x) \le S_i^U, \quad i = 1, 2, ..., m \\ & X_j^L \le x_j \le X_j^U, \quad j = 1, 2, ..., n \end{array}$$

where $f(x)$ is the objective function of independent variable x and represents the best performance that must be achieved. In a general optimization problem, the objective is to minimize the objective function. However, if the aim is to maximize the objective function, a new objective function can be set to take the negative number or the reciprocal of the original objective function.

In the equation, x denotes the independent variables in the design optimization, known as design variables, which indicate that certain parameters must be modified or adjusted. These design variables are subject to lower and upper limits, X^L and X^U, respectively.

In addition, $s(x)$ denotes the state variables that change during optimization processes depending on the design variables. The state variables indicate the reactions of the test structure after loading and are also bounded by lower and upper limits, S^L and S^U, respectively.

By using design optimization, this FEA study obtained a specific conical angle that minimizes abutment stress and represents the highest connection stability for the lowest abutment fracture possibility in the Ankylos-based conical implant–abutment connection system. In addition, the optimal conical angle of the optimal design was compared with that of the original design to determine the extent of improvement.

Materials and Methods

Finite element models

Finite Element Model Design

In this study, we used ANSYS 11.0 to develop the finite element (FE) model and to perform FE analyses and optimization

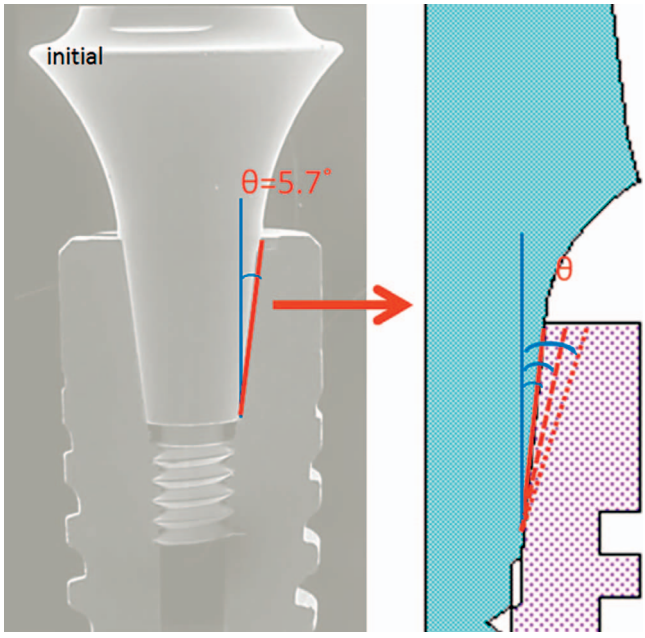

Figure 2. Conical half angle h is the design variable, and it controls the diameter of the abutment and thickness of the corresponding implant wall. A h of 5.78 represents the original design of the Ankylos implant system.

iterations. The 3-dimensional FE model comprised a superstructure, abutment, implant and bony block. In the aforementioned clinical failure cases, the geometries of an Ankylos B11 implant (diameter: 4.5mm; length: 11mm) and a standard C/ abutment (b/1.5/6.0 straight) were used as references for FE models of the implant and abutment parts. In particular, because the aim of this study was to obtain the optimal conical angle through optimization iterations, we set the conical half angle θ as the design variable. Other related conical connection parts were built according to the variation of this variable. A θ of 5.7° represented the original design of the Ankylos implant system (Figure 2). In addition, to simplify the modeling, the threads of the implant body and abutment screw were not represented as spirals but as symmetrical rings.[26,27]

For FE model validation with in vitro tests, the geometries of the bony block and superstructure were modeled using cuboid blocks, which allowed a firm fixation of samples and a stable loading point in the experimental settings.[28] The bony block was 17 × 17 × 15 mm^3 in size and included a 1.5-mm cortical layer. The superstructure was 11 × 11 × 10 mm^3 in size with a 60° inclined plane on the top for fulfilling the following loading conditions.

The FE model was developed using SOLID187 with 10-node tetrahedral elements that are suitable for developing meshes on irregular bodies.[28] In total, the FE model comprised 603 406 nodes and 386 044 elements (Figure 3).

Material Properties

All materials were assumed to be linearly elastic, homogeneous, and isotropic. The implant was made of titanium, and the superstructure and abutment were made of a titanium alloy. Poly(methyl methacrylate) (PMMA) and stainless steel were used to replace the bone to validate the FE models in the corresponding in vitro test. The properties of the materials are listed in Table 1.

Interface Conditions

The bone–implant interface (which simulates 100% osseointegration), superstructure–abutment interface, and cortical–cancellous bone interface were assumed to be completely bonded.

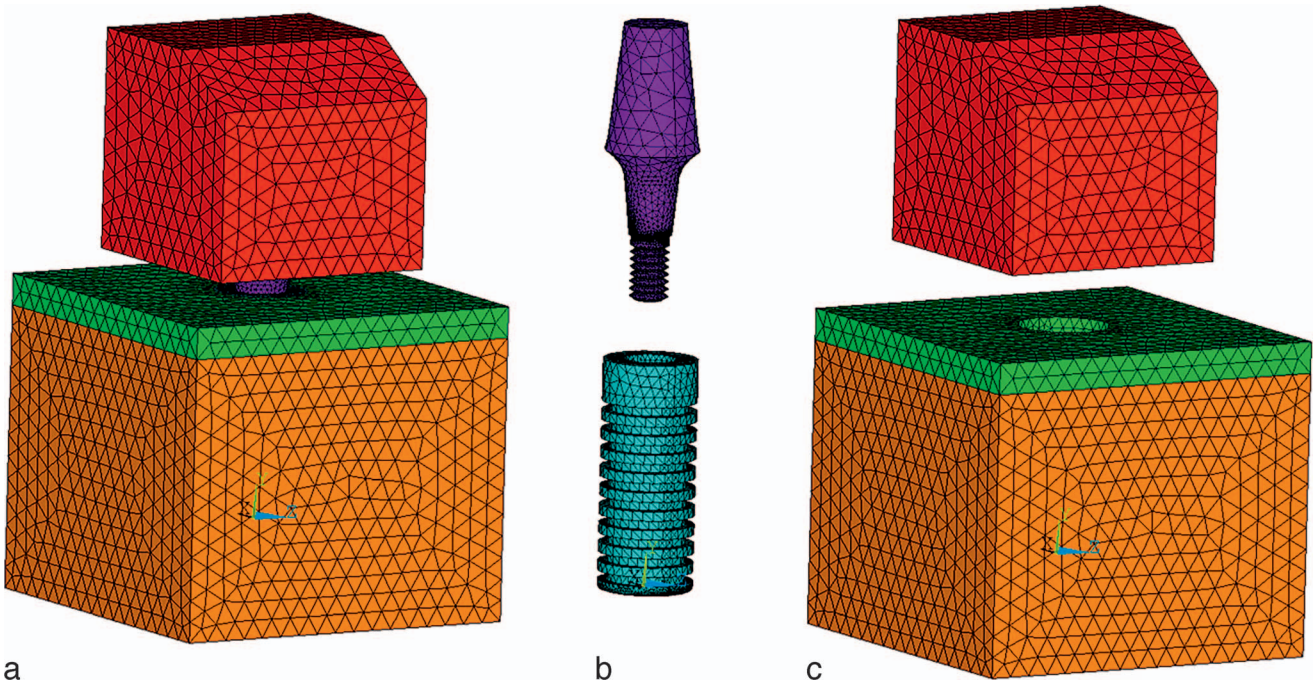

Figure 3. Finite element (FE) models with a mesh construction. (a) Complete FE model. (b) Models of the abutment and implant. (c) Models of the superstructure and bony block.

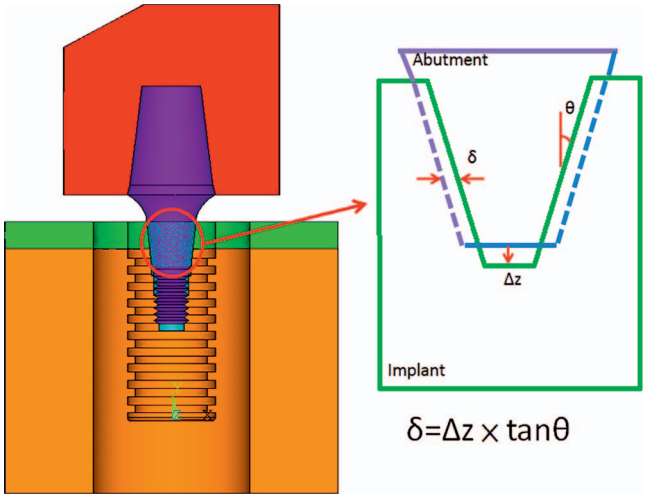

Figure 4. Cross-sectional view of an FE model showing details of the implant abutment connection. The right diagram demonstrates the interference in the implant abutment connection, defined by $\theta = \Delta z \times \tan\theta$ (where θ is the interference value, Δz is the axial displacement, and θ is the conical half angle).

To simulate real behavior at the abutment and implant interface, an interference value should be imported into FE models. In other words, at the same level, the dimension of the abutment should be slightly larger than that of the implant bore by the interference value. This results in overlapping of the contact boundaries. However, in reality, the interference value (δ) is too small to be directly measured; therefore, it is calculated using the formula $\delta = \Delta z \times \tan\theta$, where Δz is the axial displacement and θ is the conical half angle (Figure 4).[13]

In our study, axial displacement (Δz) of the abutments after the application of 25 Ncm torque, as recommended by the manufacturer, was measured in vitro (averaging 25 μm), and the data were applied to the formula $\delta = 25 \times \tan(5.7°)$. The interference value was approximately 2.5 μm and was imported into the FE models. Nonlinear contact with friction was assumed between the abutment and implant in the conical interface, and the abutment–implant conical contact was modeled using elastic surface-to-surface contact elements (conta174 and targe170). The friction coefficient (μ) adopted for the conical interface was 0.3.[16]

Loading and Boundary Conditions

To simulate the conditions of human mastication in the posterior area, a 30° off-axis loading of 200 N was applied eccentrically 4 mm to the right of the center of the superstructure and 10.5 mm above the platform of the implant (Figure 5a).[36] The generated axial loading, bending moment, and counterclockwise torsional moment was 173.2 N, 105 Ncm, and 40 Ncm, respectively. Additionally, the models were constrained in all directions at the nodes on the mesial, distal, and lower bone surfaces (Figure 5b).

FE model validation

In the experimental test, each implant was embedded in PMMA (Hygenic Repair Acrylic, Coltene/Whaledent, Langenau, Germany) and confined to the center of a stainless steel form.[37] The corresponding abutment was connected to the implant and tightened at 25 Ncm. A titanium superstructure was then cemented onto the abutment with resin-modified glass ionomer luting cement (RelyX Luting 2 cement; 3M ESPE, St Paul, Minn). The implant–abutment assemblies were consistent with those used in the aforementioned FE models. The titanium superstructure and stainless steel form corresponding to the bone block in the FE models in this study were developed using CAD/CAM according to the dimensions of the FE models.

A specimen was subjected to a 90° off-axis load on the lateral surface of the superstructure, 10.5 mm above the platform of the implant (Figure 6a). The load test was performed using a universal testing machine (ElectroForce 3200; Bose, Eden Prairie, Minn). A 1-N preload was applied prior to the test load from 0 to 155 N at a crosshead speed of 15 N/s. Load–displacement curves were recorded, and the stiffness was calculated, followed by the calculation of the displacement value under 100 N.

For validation, the FE models were slightly modified by changing the loading condition and material properties of the PMMA and stainless steel corresponding to the experimental test (Figure 6b). The loading magnitude was set to 100 N, and the displacement of the loading point was recorded. A comparison of the experimental outcomes was performed to validate the accuracy of the models.

Optimization analysis

To obtain the highest connection stability for the lowest abutment fracture possibility, an objective function $f(x)$ was set to determine the minimal abutment stress. In this study, the stress status of the abutment was represented by the maximum von Mises stress in the abutment, which was defined as the state variable.

The design variable θ was the conical half angle. By fixing the bottom radii of the conical portion of the abutment, the entire conical portion increases as θ increases, and the thickness of the corresponding implant wall consequently decreases; moreover, θ was set to a range between 1.5° and 16°. Notably, an initial value must be applied for an initial analysis before running the optimization algorithm. Based on the original design of the Ankylos system, the initial value of θ was set to 5.7° (Figure 2).

In every optimization iteration, every state variable obtained, depending on its corresponding design variable, was the maximum von Mises stress in the abutment. To ensure the rigidity of the abutment and implant, the boundary of the state variable was set to below the ultimate tensile strength of the titanium alloy (910 MPa).[38] Therefore, the objective function was to obtain the minimized state variable.

This study performed an optimization algorithm by using the subproblem approximation method. This method can be described as an advanced, zero-order method. A convergence tolerance of 0.001 was provided in the program.

Comparison of the optimal and original designs

The optimal design was compared with the original design in terms of several postprocessing FE results to establish the

Table 1

Mechanical Properties used in the finite element analyses

Material	Young's Modulus (E) (MPa)	Poisson's Ratio (ν)	References
Titanium	110 000	0.35	Benzing et al,[29] Chang et al[30]
Titanium alloy (Ti-6Al-4V)	110 000	0.35	Saidin et al[31]
Cortical bone	13 700	0.3	Pessoa et al[32]
Cancellous bone	1370	0.3	Pessoa et al,[32] Meijer et al[33]
Acrylic resin (poly[methyl methacrylate])	1500	0.35	Hatamleh et al[34]
Stainless steel	200 000	0.31	Yaman et al[35]

extent of improvement. First, the maximum von Mises stress values in the abutment and implant were examined to elucidate their abilities to resist structure fracture. Second, the maximum values and the distribution of the contact pressure in the connection were examined to represent the conditions of the clamping force in the connection. Then, the maximum values of the microgap at the implant–abutment interface were examined, which could be indices for the performance of the connection stability during loading and the health of tissues around the connection. Finally, the maximum values of the principal stress of the cortical bone were examined to elucidate the stress status of the surrounding bone.

Results

FE model validation

The experimentally measured and numerically calculated displacement values at the same loading point were 0.33 and 0.28 mm, respectively, indicating a reasonable model validation.

According to the results of the initial value (5.7°), the maximum von Mises stress occurred on the abutment at the implant platform level, consistent with the abutment fracture area observed clinically (Figure 1a and b). These corresponding findings can also be used for FE model validation.

Optimization analysis

This optimization process comprised 5 iterations, each of which is shown in Figure 7. The optimal conical half angle was calculated to be 10.1°.

Comparison of the optimal and original designs

A comparison of the original and optimal designs is presented in Table 2. Notably, the optimal design exhibited reduced maximum von Mises stress in both the abutment and implant by 36.4% and 25.5%, respectively. Because the maximum von Mises stress of the abutment was reduced from 683.70 to 434.73 MPa, the abutment of the optimal design significantly reduced fracture probability. The same positive effect occurred in the implant of the optimal design.

In terms of clamping force in the connection, although the maximum contact pressure in the connection of the optimal design was reduced by 37.9%, a more uniform stress distribution was observed (Figure 8). The maximum microgap at the implant–abutment interface of the optimal design was reduced by 62.3%, indicating significant improvement in the connection stability. The reduced microgap also contributes to the health of the surrounding tissue. In addition, the maximum principal stress of the cortical bone in the optimal design was reduced by 4.5%, indicating that the optimal design is beneficial to the maintenance of the surrounding cortical bone.

Discussion

In this study, 3-dimensional FE models were experimentally validated before optimization processes were conducted. Because the displacement value measured in the experimental test was very close to the value of the FEA estimate, the accuracy and rationality of these FE models was confirmed. Nevertheless, the displacement value calculated from the FE models was lower than the actual experimentally measured value. The cause of this negative deviation may have been the discrepancy between the perfect assumption of linear elasticity, homogeneity, and isotropism in the FE models and the imperfect conditions in the setup of the experimental tests due to experimental errors.

In terms of FE modeling, the interference phenomenon (an important characteristic of conical connections) was simulated and imported into the FE models; notably, in most FEA studies, this phenomenon has been neglected. In addition, the use of simplifying threads on the implant body and the abutment screw in the models to conserve computational resources in the execution of optimization calculations and to facilitate mesh construction was proved feasible by the positive validation result.

The conical angle was considered to be the key parameter influencing the dynamic stability of the conical connections.[39] In the analysis of the clinical failure cases, the conical angle exerted opposing effects on abutment rigidity and frictional resistance in the connection. Therefore, in this study, the conical angle was set as the design variable to determine the value that would create the highest connection stability. In addition to the conical angle, the mechanical behaviors of conical connections were determined using material properties, the coefficient of friction, the depth of insertion (interference), and geometric factors that include contact length and inner and outer diameters of the members.[13] Because of the heterogeneity of different implant systems, not all of these parameters in every implant system are consistent; we therefore used the Ankylos implant system analysis cases as a reference in this pilot study to control them. We suggest that additional studies on different conical connection systems

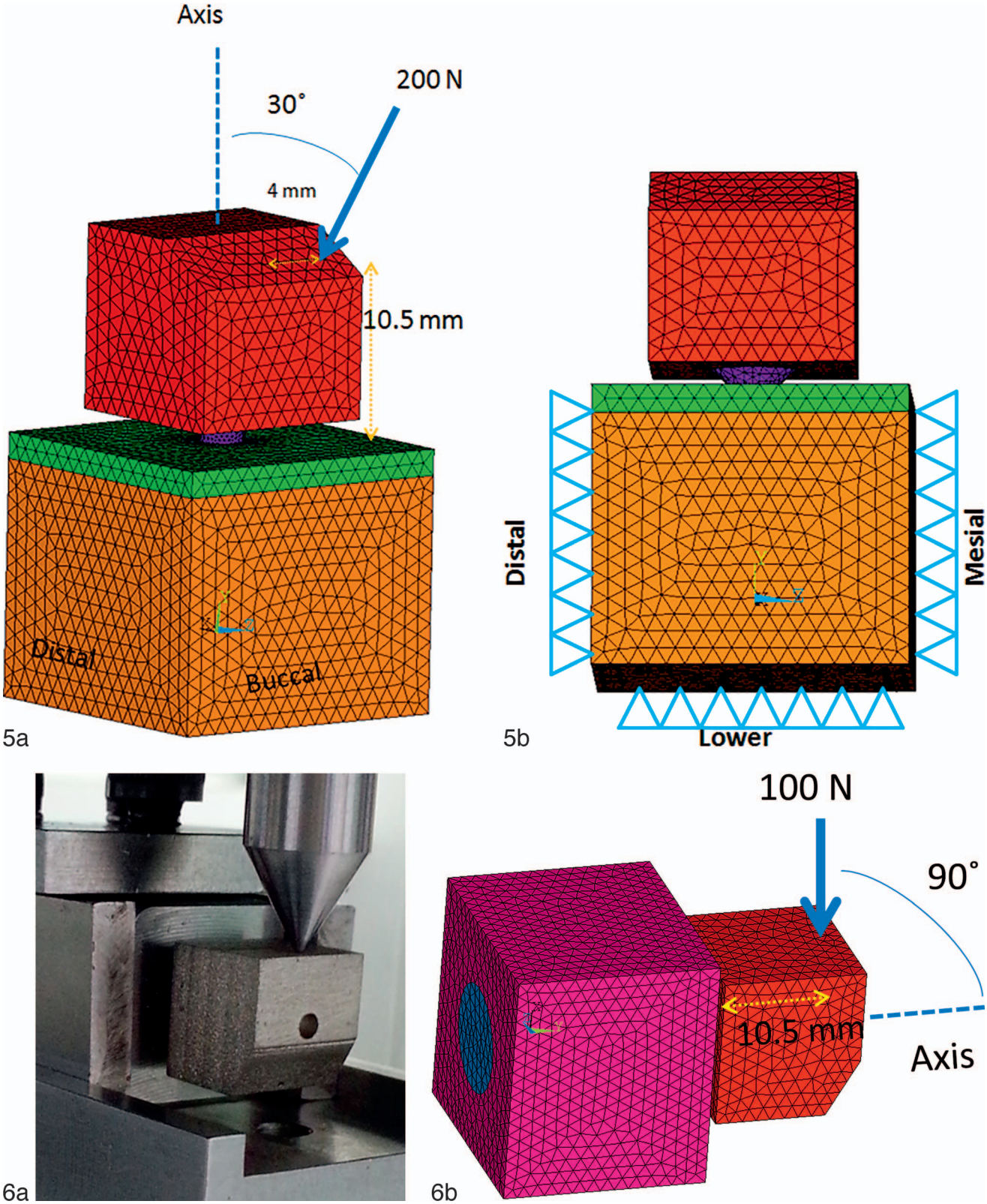

Figures 5 and 6. Figure 5. Loading and boundary conditions in the finite element analysis. (a) Loading conditions in the optimization analysis simulating posterior occlusion in the oral cavity. (b) Boundary conditions. **Figure 6.** Finite element model validation. (a) Experimental test setup for validation. (b) Loading conditions corresponding to the experimental test in the finite element model for validation.

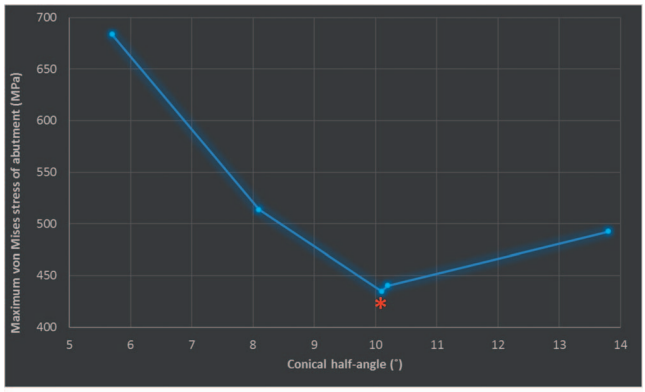

Design variable	Conical half-angle (°)	5.7	8.1	10.1	10.2	13.8
State Variable	Maximum von Mises stress of abutment (MPa)	683.70	513.61	434.73*	440.30	492.42

Figure 7. Line graph composed of all optimization iterations (blue point), which are also listed in the lower table. The graph reveals the relationship between the maximum von Mises stress in the abutment and conical half angle. The asterisk indicates the optimal conical half angle (10.1°) at which the value of the maximum von Mises stress of the abutment was minimal (434.73 MPa).

should be conducted to define the optimal conical angle in various conical connection designs.

In the original design, the maximum von Mises stress (683.70 MPa) occurred in the abutment at the implant platform level, consistent with clinical findings. The value of 683.70 MPa was below the ultimate tensile strength of the titanium alloy, which was 910 MPa. Therefore, the incidence of abutment fracture is clinically rare. However, under the fatiguing effects of chewing or unfavorable parafunctions such as bruxism and clenching, abutment fracturing may occur.[15] In the optimal design, the maximum von Mises stress of the abutment was 434.73 MPa, which was the minimal value in all optimization iterations. Because this is the lowest value compared with the ultimate tensile strength of the titanium alloy, the probability of abutment fracture could be the lowest. Therefore, the optimal design has the highest chance of solving the problem of abutment fracture in the Ankylos implant system.

According to the objective function in this design optimization, the obtained optimal design possessed the highest connection stability, resulting in minimal abutment stress. Compared with the original design under the same loading conditions, the higher connection stability contributed to a more uniform distribution of the contact pressure in the connection, which further led to lower values of the maximum von Mises stress of both the abutment (36.4%) and the implant (25.5%), a lower microgap at the implant–abutment interface (62.3%) and a lower maximum principle stress in the cortical bone (4.5%). In sum, the substantial improvement in all comparisons indicated that this optimization study had a important clinical value. Therefore, future research should focus on making a real product based on the optimization design and comparing it with the original product to prove its value in clinical applications.

The relationship between connection stability and the conical angle in the conical implant–abutment connection is presented in the line graph in Figure 7, in which the relationship between the conical half angle and maximum von Mises stress in the abutment (a valid indicator of connection stability) was predicted through the optimization process. Two stages with opposing trends were observed. At the first stage, when the conical half angle was below 10.1°, the connection stability increased with an increase in conical half angle. This is possibly attributable to the fact that the stiffer abutment helped overcome the negative effects of the decreased clamping force and the decreased implant rigidity. In other words, in terms of overall connection stability, the role of abutment rigidity was more critical than that of implant rigidity and clamping force. At the second stage, when the conical half angle was above 10.1°, the connection stability decreased with an increase in the conical half angle. This was possibly a result of both the abutment rigidity and conical half angle increasing, which prevented the connection from overcoming the negative effects of the decreased clamping force and implant rigidity, and thus resulted in a decreased connection stability.

The magnitude of stress and its distribution were considerably influenced by loading conditions in the FE analysis; therefore, the setting of loading conditions was an essential factor in this study. Based on scanning electron microscopy observations of clinical failures (Figure 1c), the end of the fracture was not exactly opposite the fracture origin, and the directions of the crack propagation were multiple. These findings indicated that the abutment withstood not only bending forces but also torsional forces, consistent with chewing patterns in the posterior area.[36,40] In addition, failure was observed in all the posterior restoration cases. Therefore, the loading condition, comprising force magnitude and force moments, was set in accordance with the posterior occlusion in the oral cavity in this study.

From a mechanical engineering perspective, the clamping force in conical connections originates from a large frictional resistance. Because the diameter of the male cone is slightly

Table 2

Comparison of the original and optimal designs

	Original Design	Optimal Design	Difference
Conical half-angle	($\theta = 5.7°$)	($\theta = 10.1°$)	
Maximum von Mises stress of abutment	683.70 MPa	434.73 MPa	–36.4%
Maximum von Mises stress of implant	504.81 MPa	376.26 MPa	–25.5%
Maximum principal stress of cortical bone	36.60 MPa	34.97 MPa	–4.5%
Maximum microgap between implant-abutment connection	2.75 μm	1.04 μm	–62.3%
Maximum contact pressure in the connection	514.20 MPa	319.23 MPa	–37.9%

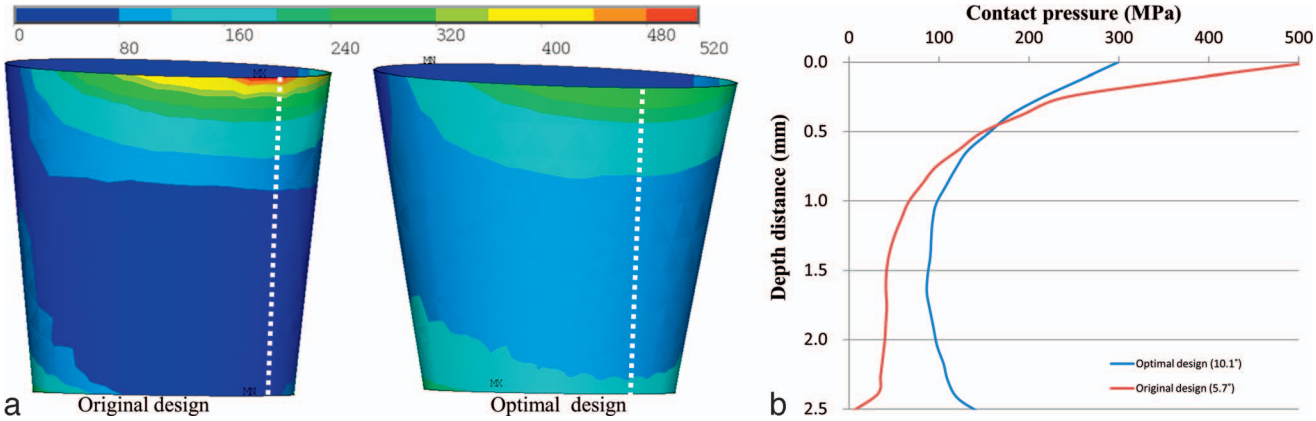

Figure 8. Distribution of contact pressure. (a) Distribution of contact pressure in the implant–abutment connection for the original and optimal designs. (b) Illustration of pressure amplitudes with the depth distance from the platform to the cone bottom corresponding to the white dotted lines marked in (a). The optimal design demonstrated lower maximum pressure values and more uniform pressure distribution.

larger than that of the female receptacle at the same level, a wedge effect occurs. Contact pressure is subsequently generated on both surfaces when the male cone is fitted into the female element.[10] Therefore, the discrepancy between the abutment and implant bore at the same level, defined as interference (δ), is characteristic of conical connections.

To simulate real behavior, an interference value and its contact elements were imported into the FE models. Because of this phenomenon, contact pressure was generated in the connection while screwing and was transformed into a clamping force that stabilized the connection prior to occlusal loading. However, the contact pressure within the connection led to internal stressing of the abutment and implant, which increased with a decrease in the conical angle. In the original design, a smaller conical angle resulted in the storage of a larger contact pressure in the connection. Therefore, under the same loading conditions, the stresses on the implant and abutment were higher in the original design compared with the optimal design. Consequently, a larger clamping force in the connection is not necessarily more effective than a smaller one. In fact, the optimal value is the appropriate value, not the largest value. An appropriate clamping force in the connection contributes to low stress on implant components and facilitates retrieval in case of abutment fracture.

In engineering, design optimization is an advanced concept because optimization requires tedious mathematical operations. An FE model combined with optimization analysis is an effective simulation tool for facilitating the design of medical devices, such as spinal cages,[41] thumb spica splints,[42] spinal braces,[43] and implants.[44] In this study, this methodology helped improve a current implant product on the market by enhancing its durability. Through an analysis of failed retrieval cases, this study can provide researchers with in-depth information to determine the possible causes of failure. The conical angle was set as a design variable to be optimized. By using design optimization, the optimal angle was calculated using the conditions of the objective demands and material constraints, which is more convincing compared with the determination by skilled designers based on their knowledge, experience, and judgment. Furthermore, manufacturers of individual implant systems can continuously improve their systems' performance according to specific clinical problems by using the method in this study.

Conclusion

Within the limitations of this study, the optimal design of the Ankylos-based implant system (conical half angle = 10.1°) was determined using design optimization, which proved to not only reduce the possibility of abutment fracture but also increase the longevity of the implant therapy overall. Because of the heterogeneity of different systems, we suggest that additional studies be conducted to define the optimal conical angle in various conical connection designs.

Abbreviation

CAD: computer-aided design
CAM: computer-aided manufacturing
FE: finite element
FEA: finite element analysis
PMMA: poly(methyl methacrylate)

Acknowledgment

This study was supported by a research grant (MOST 103-2314-B-010-023) from the Ministry of Science and Technology in Taiwan.

Note

The authors declare that they have no conflicts of interest.

References

1. Romeo E, Lops D, Margutti E, Ghisolfi M, Chiapasco M, Vogel G. Long-term survival and success of oral implants in the treatment of full and

partial arches: a 7-year prospective study with the ITI dental implant system. *Int J Oral Maxillofac Implants*. 2004;19:247–259.

2. Adell R, Lekholm U, Rockler B, Branemark PI. A 15-year study of osseointegrated implants in the treatment of the edentulous jaw. *Int J Oral Surg*. 1981;10:387–416.

3. Goodacre CJ, Kan JY, Rungcharassaeng K. Clinical complications of osseointegrated implants. *J Prosthet Dent*. 1999;81:537–552.

4. Jung RE, Pjetursson BE, Glauser R, Zembic A, Zwahlen M, Lang NP. A systematic review of the 5-year survival and complication rates of implant-supported single crowns. *Clin Oral Implants Res*. 2008;19:119–130.

5. Binon PP. The effect of implant/abutment hexagonal misfit on screw joint stability. *Int J Prosthodont*. 1996;9:149–160.

6. Binon PP, McHugh MJ. The effect of eliminating implant/abutment rotational misfit on screw joint stability. *Int J Prosthodont*. 1996;9:511–519.

7. Schmitt CM, Nogueira-Filho G, Tenenbaum HC, et al. Performance of conical abutment (Morse Taper) connection implants: a systematic review. *J Biomed Mater Res A*. 2014;102A:552–574.

8. Norton MR. An in vitro evaluation of the strength of an internal conical interface compared to a butt joint interface in implant design. *Clin Oral Implants Res*. 1997;8:290–298.

9. Khraisat A, Stegaroiu R, Nomura S, Miyakawa O. Fatigue resistance of two implant/abutment joint designs. *J Prosthet Dent*. 2002;88:604–610.

10. Bozkaya D, Muftu S. Efficiency considerations for the purely tapered interference fit (TIF) abutments used in dental implants. *J Biomech Eng*. 2004; 126:393–401.

11. Akca K, Cehreli MC. A photoelastic and strain-gauge analysis of interface force transmission of internal-cone implants. *Int J Periodontics Restorative Dent*. 2008;28:391–399.

12. Kitagawa T, Tanimoto Y, Murakami H, et al. Evaluating the dynamic behavior of taper joint implants under different loading conditions: a transient dynamic finite element analysis. *Int J Oral Med Sci*. 2013;12:105–111.

13. Bozkaya D, Muftu S. Mechanics of the tapered interference fit in dental implants. *J Biomech*. 2003;36:1649–1658.

14. Krebs M, Schmenger K, Neumann K, Weigl P, Moser W, Nentwig GH. Long-term evaluation of ANKYLOS dental implants, part I: 20-year life table analysis of a longitudinal study of more than 12,500 implants. *Clin Implant Dent Relat Res*. 2015;17:e275–e286.

15. Romanos GE, Nentwig GH. Single molar replacement with a progressive thread design implant system: a retrospective clinical report. *Int J Oral Maxillofac Implants*. 2000;15:831–836.

16. Streckbein P, Streckbein RG, Wilbrand JF, et al. Non-linear 3D evaluation of different oral implant-abutment connections. *J Dent Res*. 2012; 91:1184–1189.

17. Shim HW, Yang BE. Long-term cumulative survival and mechanical complications of single-tooth Ankylos implants: focus on the abutment neck fractures. *J Adv Prosthodont*. 2015;7:423–430.

18. Cicciu M, Bramanti E, Cecchetti F, Scappaticci L, Guglielmino E, Risitano G. FEM and Von Mises analyses of different dental implant shapes for masticatory loading distribution. *Oral Implantol*. 2014;7:1–10.

19. Cicciu M, Maiorana C, Franceschini G. Parametric analysis of the strength in the "Toronto" osseous-prosthesis system. *Minerva Stomatol*. 2009;58:9–23.

20. Lauritano F, Runci M, Cervino G, Fiorillo L, Bramanti E, Cicciu M. Three-dimensional evaluation of different prosthesis retention systems using finite element analysis and the Von Mises stress test. *Minerva Stomatol*. 2016;65:353–367.

21. Cicciu M, Cervino G, Bramanti E, et al. FEM analysis of mandibular prosthetic overdenture supported by dental implants: evaluation of different retention methods. *Comput Math Methods Med*. 2015;2015:943839.

22. Bramanti E, Cervino G, Lauritano F, et al. FEM and Von Mises analysis on prosthetic crowns structural elements: evaluation of different applied materials. *Sci World J*. 2017;2017:1029574.

23. Cicciu M, Bramanti E, Matacena G, Guglielmino E, Risitano G. FEM evaluation of cemented-retained versus screw-retained dental implant single-tooth crown prosthesis. *Int J Clin Exp Med*. 2014;7:817–825.

24. Hsu YC, Gung YW, Shih SL, et al. Using an optimization approach to design an insole for lowering plantar fascia stress—a finite element study. *Ann Biomed Eng*. 2008;36:1345–1352.

25. Javidinejad A. Theory of parametric design optimization approach via finite element analysis. *Adv Theor Appl Mech*. 2012;5:217–224.

26. Merz BR, Hunenbart S, Belser UC. Mechanics of the implant-abutment connection: an 8-degree taper compared to a butt joint connection. *Int J Oral Maxillofac Implants*. 2000;15:519–526.

27. Iplikcioglu H, Akca K, Cehreli MC, Sahin S. Comparison of non-linear finite element stress analysis with in vitro strain gauge measurements on a Morse taper implant. *Int J Oral Maxillofac Implants*. 2003;18:258–265.

28. Sannino G, Barlattani A. Mechanical evaluation of an implant-abutment self-locking taper connection: finite element analysis and experimental tests. *Int J Oral Maxillofac Implants*. 2013;28:e17–e26.

29. Benzing UR, Gall H, Weber H. Biomechanical aspects of two different implant-prosthetic concepts for edentulous maxillae. *Int J Oral Maxillofac Implants*. 1995;10:188–198.

30. Chang CL, Chen CS, Hsu ML. Biomechanical effect of platform switching in implant dentistry: a three-dimensional finite element analysis. *Int J Oral Maxillofac Implants*. 2010;25:295–304.

31. Saidin S, Abdul Kadir MR, Sulaiman E, Abu Kasim NH. Effects of different implant-abutment connections on micromotion and stress distribution: prediction of microgap formation. *J Dent*. 2012;40:467–474.

32. Pessoa RS, Muraru L, Junior EM, et al. Influence of implant connection type on the biomechanical environment of immediately placed implants—CT-based nonlinear, three-dimensional finite element analysis. *Clin Implant Dent Relat Res*. 2010;12:219–234.

33. Meijer GJ, Starmans FJ, de Putter C, van Blitterswijk CA. The influence of a flexible coating on the bone stress around dental implants. *J Oral Rehabil*. 1995;22:105–111.

34. Hatamleh MM, Rodrigues FP, Silikas N, Watts DC. 3D-FE analysis of soft liner-acrylic interfaces under shear loading. *Dent Mater*. 2011;27:445–454.

35. Yaman SD, Alacam T, Yaman Y. Analysis of stress distribution in a maxillary central incisor subjected to various post and core applications. *J Endod*. 1998;24:107–111.

36. Yao KT, Kao HC, Cheng CK, Fang HW, Yip SW, Hsu ML. The effect of clockwise and counterclockwise twisting moments on abutment screw loosening. *Clin Oral Implants Res*. 2012;23:1181–1186.

37. Yao KT, Kao HC, Cheng CK, Fang HW, Huang CH, Hsu ML. The potential risk of conical implant-abutment connections: the antirotational ability of Cowell implant system. *Clin Implant Dent Relat Res*. 2015;17:1208–1216.

38. Cordeiro JM, Barao VA. Is there scientific evidence favoring the substitution of commercially pure titanium with titanium alloys for the manufacture of dental implants? *Mater Sci Eng C Mater Biol Appl*. 2017;71: 1201–1215.

39. Kitagawa T, Tanimoto Y, Nishiyama N, Aida M. Application of finite element analysis for taper implant-abutment joints in dental implant systems. *Int J Oral Med Sci*. 2008;7:1–6.

40. Lundeen HC, Gibbs CH. Jaw movements and forces during chewing and swallowing and their clinical significance. In: Lundeen HC, Gibbs CH, eds. *Advances in Occlusion*. Boston: John Wright; 1982:2–32.

41. Zhong ZC, Wei SH, Wang JP, Feng CK, Chen CS, Yu CH. Finite element analysis of the lumbar spine with a new cage using a topology optimization method. *Med Eng Phys*. 2006;28:90–98.

42. Huang TH, Feng CK, Gung YW, Tsai MW, Chen CS, Liu CL. Optimization design of thumbspica splint using finite element method. *Med Biol Eng Comput*. 2006;44:1105–1111.

43. Liao YC, Feng CK, Tsai MW, Chen CS, Cheng CK, Ou YC. Shape modification of the Boston brace using a finite-element method with topology optimization. *Spine*. 2007;32:3014–3019.

44. Chang CL, Chen CS, Huang CH, Hsu ML. Finite element analysis of the dental implant using a topology optimization method. *Med Eng Phys*. 2012;34:999–1008.